



# Ceramic laminates with tailored residual stresses

A. J. SÁNCHEZ-HERENCIA, C. BAUDÍN

Instituto de Cerámica y Vidrio (CSIC). C. Kelsen 5. 28049 Madrid (España)

Severe environments imposed by new technologies demand new materials with better properties and ensured reliability. The intrinsic brittleness of ceramics has forced scientists to look for new materials and processing routes to improve the mechanical behaviour of ceramics in order to allow their use under severe thermomechanical conditions. The laminate approach has allowed the fabrication of a new family of composite materials with strength and reliability superior to those of monolithic ceramics with microstructures similar to those of the constituent layers. The different ceramic laminates developed since the middle 1970's can be divided in two large groups depending on whether the development of residual stresses between layers is the main design tool. This paper reviews the developments in the control and tailoring of residual stresses in ceramic laminates. The tailoring of the thickness and location of layers in compression can lead to extremely performing structures in terms of strength values and reliability. External layers in compression lead to the strengthening of the structure. When relatively thin and highly compressed layers are located inside the material, threshold strength, crack bifurcation and crack arrest during fracture occur.

*Keywords: Ceramic laminates, Fracture, Residual stress, Damage tolerance.*

## **Materiales cerámicos laminados con tensiones residuales controladas**

Las severas condiciones de trabajo de las nuevas aplicaciones tecnológicas exigen el uso de materiales con mejores propiedades y alta fiabilidad. La potencialidad de uso de materiales frágiles, como los cerámicos, en estas aplicaciones exige el desarrollo de nuevos materiales y métodos de procesamiento que mejoren su comportamiento mecánico. El concepto de material laminado ha permitido la fabricación de una nueva familia de materiales con tensiones de fractura y fiabilidad superiores a las de materiales monolíticos con microestructuras similares a las de las láminas que conforman el laminado. Los distintos materiales laminados desarrollados desde mediados de los años 70 se pueden dividir en dos grandes grupos, dependiendo de si el concepto básico para su diseño es el desarrollo de tensiones residuales en las láminas o cualquier otro concepto. En este artículo se revisan los avances en el ámbito de los materiales laminados diseñados utilizando las tensiones residuales como principal herramienta de diseño. La manipulación del espesor y la posición en el laminado de láminas en compresión puede dar lugar a estructuras con excelente comportamiento mecánico en términos de tensión de rotura y fiabilidad. Los laminados cuyas láminas externas están en compresión presentan altos valores de la tensión de fractura. Si se utilizan laminas finas sometidas a altos valores de compresión en el interior de las estructuras se pueden obtener valores umbrales de la tensión de fractura, bifurcación de la grieta y frenado de la grieta

*Palabras clave: Materiales cerámicos laminados, fractura, tensiones residuales, tolerancia al daño*

## **1. INTRODUCTION**

Severe environments imposed by new technologies demand new materials with better properties and ensured reliability. Consequently, ceramics have been proposed for use as either substitutes for current materials (e.g: metals or polymers) or as additions to existing materials (i.e. as constituents of composites), due to their favourable properties such as high hardness and compressive strength, and good thermal and chemical stability. However, the intrinsic brittleness of ceramics has forced scientists to look for new materials and processing routes to improve the mechanical behaviour while maintaining low cost and assuring low environmental impact. In the past, much of the effort to improve the mechanical behaviour of ceramics was placed in producing the highest degree of homogeneity in bulk monophase ceramics with very small flaws. However, in the last two decades new strategies fundamentally different from the conventional

“flaw elimination” approach of monolithic ceramics have emerged directed to achieve “flaw tolerance”. In this sense, laminar ceramic composites have received a great deal of attention due to their potential for use in emerging structural applications demanding high mechanical performance. The laminated approach has allowed the fabrication of a new family of composite materials with properties superior to those of monolithic ceramics with microstructures similar to those of the constituent layers. In general, the enhanced mechanical behaviour exhibited by these composites cannot be attributed to a simple rule of mixtures of the properties of the constituent materials, but to the synergic effect of the laminar structure itself.

The different ceramic laminates developed since the middle 1970's can be divided in two large groups depending on whether the development of residual stresses between layers

is the main design tool. Nature offers a number of residual stresses-free simple layered structures, such as shells or teeth, which present improved failure behaviour as compared to that of the individual components. For example, layers of stiff, hard, and brittle aragonite platelets held together by an easily to deform and tough proteinaceous matrix make nacre a rigid material in which both toughness and strength are significantly higher than those of aragonite, which constitutes the 95 vol.% of nacre. Several mechanisms leading to energy dissipation have been identified to occur during the fracture of nacre<sup>1,2</sup>: sliding of the aragonite layers, stretching of the filaments in the proteinaceous matrix and crack deflection around the aragonite plates.

Since the seminal work by Clegg et al.<sup>3</sup>, ceramic-ceramic layered composites have been designed and processed on the basis of weak interfaces between dense and rigid layers to originate crack deflection and their fracture behaviour in flexure under loads perpendicular to the layers has been analysed in terms of crack propagation and strength (e.g. see refs.<sup>4,7</sup>). Alternative ways to produce crack deflection are those incorporating different kinds of weak layers such as porous layers<sup>8</sup>, layers containing oriented microcracks<sup>9,10</sup> or heterogeneous layers introduced during the green processing<sup>11-13</sup> or formed in-situ during sintering<sup>14</sup>. In general this family of residual stress free laminates presents graceful fracture together with strength values of the same order as those of the stiff and dense layers. In figure 1, a characteristic fracture surface showing crack deflection and branching and a load-displacement plot for a laminate presenting graceful fracture is shown<sup>12</sup>.

The other large group of ceramic laminates includes those designed on the basis of the development of residual stresses between the layers during cooling from the sintering temperature. When the external layers of the laminate are in compression, large improvements in strength can be achieved especially in systems such as alumina/zirconia in which high residual stresses can be attained. This is the so called strengthening approach, similar to that traditionally used in reinforced glass. Moreover, R-curve behaviour revealing flaw tolerance is also observed in this kind of laminates for flaws embedded in the external layer<sup>15</sup>. A challenging approach is that of layered ceramics with the external layers in tension which present extreme reliability because of crack bifurcation when loaded in flexure with loads perpendicular to the layers<sup>16</sup> and threshold strength for both orientations of the load, perpendicular and parallel to the plane of the layers<sup>17-20</sup>.

Layered ceramics designed on a residual stress approach will be deeply analysed in this work. The most important design parameters for laminates are composition, thickness, number and position of the layers, which requires processing techniques capable of controlling them while maintaining the adequate joining between layers and impeding cracking and delamination. In this sense colloidal processing techniques have been widely used for green forming due to their versatility and reliability<sup>21,22</sup>. On the one hand, as the different layers are processed from discrete slurries with known composition, colloidal techniques assure the precise compositional control. On the other, intimate joining between layers in the green bodies is achieved due to the fluid character of the slurries. Moreover, the thickness of the layers can be controlled from few microns to several hundreds by an adequate selection of the method<sup>15,23-25</sup>. The colloidal processing techniques reported

for the fabrication of laminated ceramics include tape-casting<sup>9,15,26-28</sup>, centrifugal casting<sup>29</sup>, sequential slip-casting<sup>14,24,30,31</sup>, electrophoretic deposition (EPD)<sup>11,32-34</sup>, infiltration<sup>35</sup>, painting<sup>36</sup>, and combination of several techniques like tape casting with dipping<sup>23</sup>, tape casting with EPD<sup>11</sup> or tape casting with EPD and dipping<sup>12</sup>. All of them are based on the preparation of stable slurries with specific compositions that allow the sequentially addition of one layer to a previously formed one.

Stable slurries ensure homogenous and well dispersed composition and are obtained by controlling the inter-particle potentials developed within the liquid media. The thickness of the different layers is controlled by controlling processing parameters that are characteristic for each technique (e.g.:

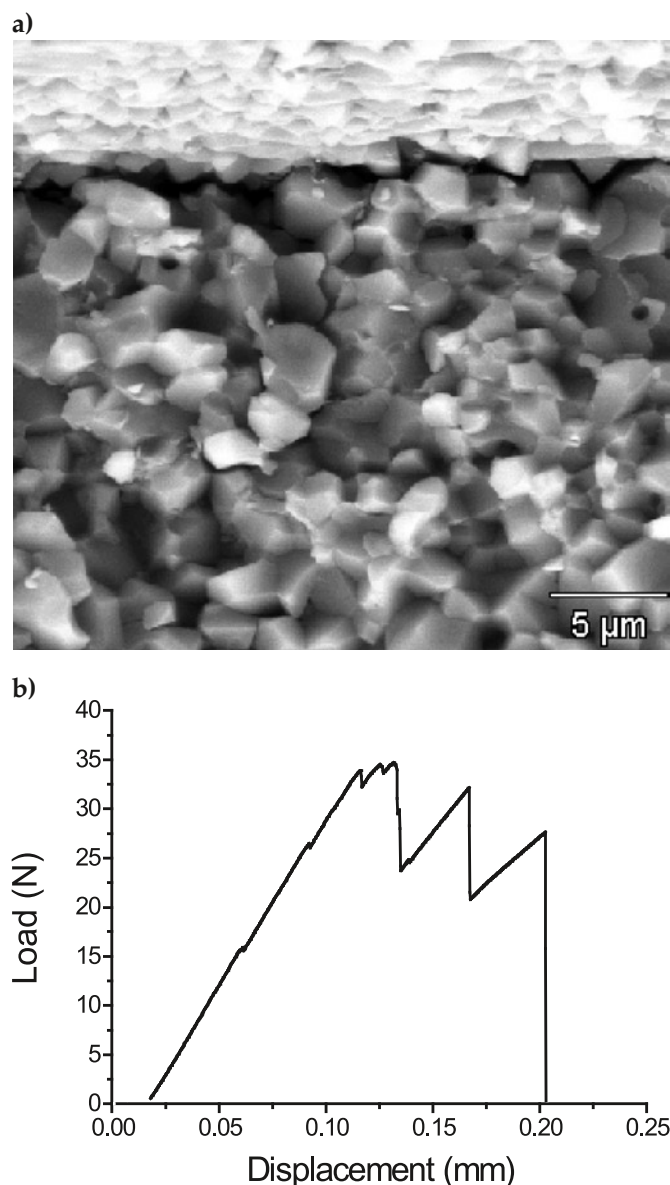


Figure 1. Alumina-aluminium titanate laminate fabricated using a combination of tape casting, dipping and EPD<sup>12</sup>.

a) Detail of crack deflection and branching through a layer. Scanning electron microscopy (SEM) micrograph of a fracture surface.

b) Characteristic plot load-displacement of the load frame presenting graceful fracture. As sintered specimens ( $\approx 35$  mm  $\times$  12 mm  $\times$  1.2 mm thick) tested in three point bending (20 mm span, 0.5 mm $\cdot$ min<sup>-1</sup>).

time for slip casting or EPD<sup>14, 24, 31, 33</sup>, the gap between the blades or the number of piled tapes for tape casting<sup>25</sup>, solid concentration in the slurry for dipping<sup>12, 23, ...</sup> etc.). Figure 2 shows two materials fabricated by tape casting and piling of tapes that illustrate the versatility of colloidal processing techniques<sup>15</sup>.

Last but not least, sintering schedules to reach co-sintering to full density of layers with different compositions and green body characteristics such as packing and particle grain size and shape have to be adjusted<sup>14, 26, 27</sup>.

## 2. RESIDUAL STRESSES IN CERAMIC LAMINATES

### 2.1. Origin of residual stresses

Commonly residual stresses arise during cooling from the sintering temperature due to the strain mismatch originated by differences in the coefficients of thermal expansion CTE ( $\alpha_i$ ) of the constituents of the layers<sup>15-17, 26, 29, 32-34, 37-40</sup>. In addition to this strain mismatch source, phase transformations ( $\Delta\epsilon_i$ )<sup>18, 23, 24, 30, 41-43</sup> or reactions ( $\Delta\epsilon_r$ )<sup>44</sup> inside the layers have to be considered. For a particular strain mismatch, the level of residual stresses is a function of the elastic constants of the constituents of the layers and the characteristics of the interface.

The total strain mismatch,  $\Delta\epsilon$ , between two given layers A and B, after cooling a certain  $\Delta T$  from a reference temperature  $T_{ref}$  down to a temperature  $T_r$  may be expressed as:

$$\Delta\epsilon = (\alpha_A - \alpha_B)\Delta T + \Delta\epsilon_t + \Delta\epsilon_r \quad (1)$$

$T_{ref}$  is the temperature above which residual stresses are negligible because the strain mismatch is accommodated by mass transport mechanisms or the reactions and/or phase transformations leading to the strain mismatch do not occur.

Compositional control to match layers with differences in  $\alpha$ <sup>15-17, 29, 32, 34, 40, 45</sup> or different amounts of transformable zirconia<sup>24, 30, 41</sup> have been employed to reach designed residual stresses in laminates. As a first approach, residual stresses can be estimated using the thermal strains and the elastic properties of monolithic materials with the same composition of the constituent layers and fabricated using the same experimental conditions, assuming that no interaction occurs at the interfaces between layers.

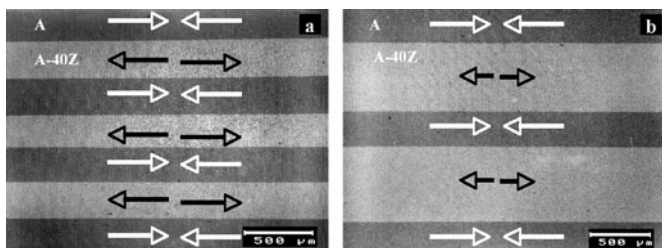


Figure 2. Two materials fabricated by cold piling and pressing of tapes fabricated by tape casting. The dark layers are constituted by alumina+5vol.%YTZP, A5Z, and the clear ones are constituted by alumina+40vol.% of YTZP, A40Z. The thin layers were formed from one tape in the green state and the thicker ones were formed from two tapes. The simplified stress state is indicated: the dark layers are in compression and the clear ones are in tension<sup>15</sup> SEMmicrographs of polished surfaces.

In figure 3 dilatometric curves recorded during cooling from the sintering temperature for two classical systems in the field of the ceramic laminates are plotted.

In figure 3 a the curves for zirconia materials with amounts of  $Y_2O_3$  ranging from pure zirconia (0%) to YTZP (3 mol%)<sup>30</sup> are shown. Significant dilatometric changes are observed in the temperature range 900-400°C due to the tetragonal-monoclinic transformation of zirconia in the materials. The total thermal strain and the temperature of the transformation decrease as the stabilizer content increases.

In figure 3 b the cooling curves from sintering for alumina with 5 vol.% (A5Z) and alumina with 40 vol.% (A40Z) of YTZP specimens are shown. In this case, the differences between the thermal expansion coefficients of YTZP ( $\alpha_{ZrO_2}$ ) and alumina, ( $\alpha_{Al_2O_3}$ )<sup>1</sup> led to higher values of strain on cooling for the of the A40Z composite than for the A5Z one and, consequently, to the  $\Delta\epsilon$  observed.

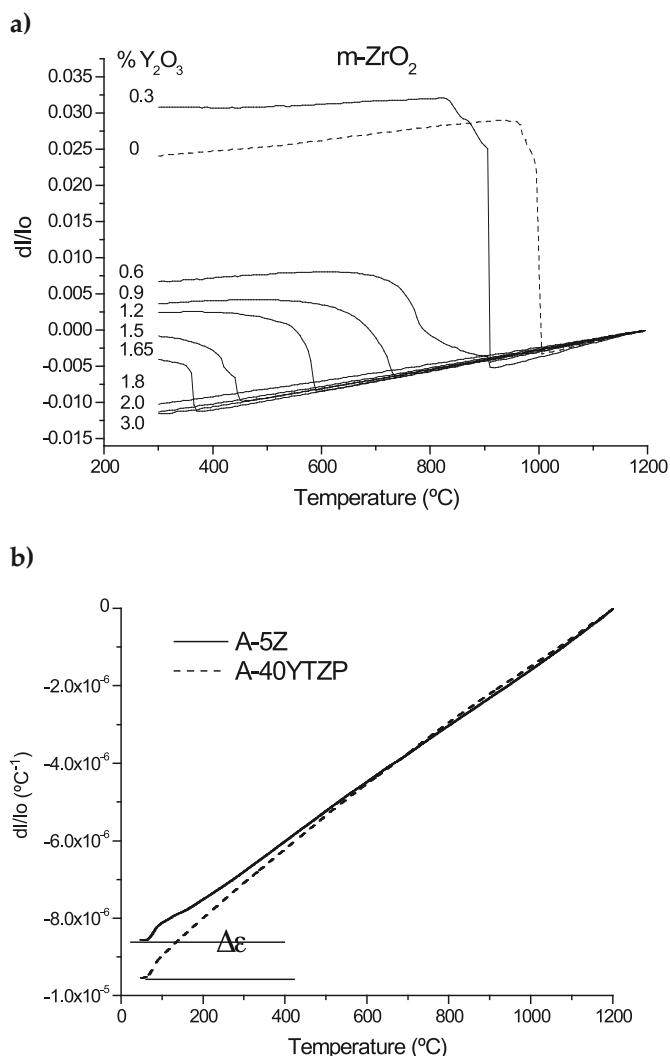


Figure 3. Dilatometric curves recorded during cooling for two compositions used in ceramic laminate designs. a) Zirconia with amounts of  $Y_2O_3$  ranging from 0 to 3 mol%. The sintered material without addition is pure monoclinic zirconia, MZ, and the sintered material with 3 mol% addition is tetragonal zirconia polycrystal, YTZP<sup>30</sup>. b) Alumina-YTZP composites with 5 and 40 vol% of YTZP. These are the compositions of the layers of the laminates shown in figure 2<sup>15</sup>.

On the basis of the dilatometric differences on cooling of different compositions such as those shown in figure 3 it is possible to design layered structures with specific strain mismatches and, consequently, with tailored levels of residual stresses through the laminate configuration.

The level and sign of the expected residual stresses in a symmetric laminate constituted by alternate layers of composition "a" and thickness  $t_a$  and layers of composition "b" and thickness  $t_b$ , can be evaluated using the simplified model of a symmetric laminate with a uniform biaxial distribution of stresses in the bulk plane of each layer and assuming an infinite body on x and z directions. This model is very useful for the design of laminates even though results are not valid near the edges because they are stress free in equilibrium and, therefore, their residual stress state is modified. The layered ceramic is considered to be in a stress-free state at the sintering temperature due to the relief of stress by mass transport mechanisms (figure 4a). During cooling from sintering, if the layers are not strongly joined the material will delaminate and each layer will shrink freely to a length dictated by equation 1. On the contrary, if the layers are strongly joined (figures 2 and 4b, c), constraint of each layer by its surrounding will result in the generation of residual stresses within the laminate.

Layers with lower CTEs or expansive phase transformations or reactions will develop compressive stresses while the adjacent layers will develop tensile stresses. Considering n layers of composition "a" and thickness  $t_a$  and (n-1) layers of composition "b" and thickness  $t_b$ , the residual stress at each layer is given by <sup>46</sup>:

$$\sigma_a = -\frac{\Delta\varepsilon \cdot E'_a}{1 + \frac{E'_a \cdot n \cdot t_a}{E'_b \cdot (n-1) \cdot t_b}} \quad (2) \quad \text{and}$$

$$\sigma_b = -\frac{\Delta\varepsilon \cdot E'_b}{1 + \frac{E'_b \cdot (n-1) \cdot t_b}{E'_a \cdot n \cdot t_a}} \quad (3)$$

where, being  $E_i$  the Young modulus and  $\nu_i$  the Poisson ratio of a given layer. Following convention, it has been assumed that compressive stresses are negative and tensile stresses are positive.

This model predicts homogeneous stress distribution across the layers and values provided by equations (2) and (3) are the maximum ones expected <sup>47,48</sup>. Combining equations 2 and 3, the stress in one layer is related to the stress in the adjacent layers by

$$\sigma_b = -\sigma_a \frac{n \cdot t_a}{(n-1) \cdot t_b} \quad (4)$$

This equation indicates that for a given thermal strain mismatch between the layers, the thickness ratio can be manipulated to develop desired stress states within the layers. It is important to notice that when very thin layers are combined with relatively thick ones ( $t_b \ll t_a$ ), the stress level inside the latter ones is negligible. As it will be discussed

later, compressive stresses are beneficial for the mechanical response as they can lead to strengthening, crack bifurcation, crack arrest and threshold strength. On the other hand, tensile stresses at the external layers of the structure decrease the strength of the material whereas tunneling cracks that can originate the failure of the structure appear when the tensile stresses overpass a critical value in the internal layers. For these reasons, and taking into account the relationship given by eq. (4) relatively thick tensile layers are usually envisaged. The optimization of laminate structure in terms of thicknesses of the layers has been analyzed by Bermejo et al <sup>49</sup>.

### 2.2 Evaluation of residual stresses

The actual residual stresses developed in a laminate depend on the properties of the constituent layers, the structure of the laminate, and the characteristics of the interfaces. In order to be able to design laminates, the residual stresses can be predicted from the properties of monolithic samples with the composition of the layers and fabricated using the same experimental conditions, and assuming that there is no interaction between the layers. As discussed above, residual stresses can be evaluated analytically using a simplified model (eqs. (2)-(3)). The main limit for this model is that it loses validity when approaching the surfaces where fracture usually initiates from critical defects. The finite element method (FEM) has been used to overcome this limit in alumina-zirconia laminates with external <sup>50</sup> and internal <sup>18</sup> compressive residual stresses. The stress profile calculated with the three-dimensional finite element model (FEM) describes the residual stress distribution through the layers both in the bulk and at the surface of the laminates. Residual stresses in the bulk calculated by FEM are practically constant within each layer and values agree with those calculated analytically.

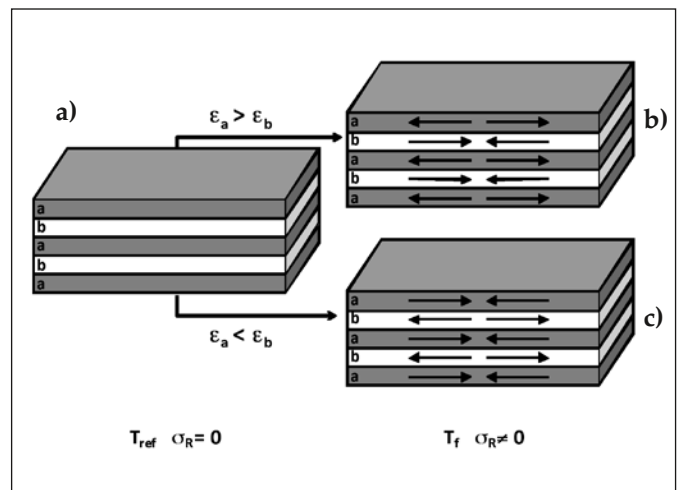


Figure 4. Simplified model of a symmetric laminate constituted by alternate layers of composition, a, and thickness,  $t_a$ , and layers of composition, b, and thickness,  $t_b$ . a) Residual stress,  $\sigma_R$ , free state at the reference temperature,  $T_{ref}$ . b) Residual stress state for thermal strain of composition a,  $\varepsilon_a$ , larger than for composition b,  $\varepsilon_b$ . "a" layers are under tension and "b" layers are under compression. c) Residual stress state for thermal strain of composition a,  $\varepsilon_a$ , smaller than for composition b,  $\varepsilon_b$ . "a" layers are under compression and "b" layers are under tension.

The assumptions used for calculations do not take into account specific microstructural developments in the layers due to the layered structure or interactions at the interfaces between the layers. In order to validate and/or to establish the applicability limits of the calculations and to deduce the expected behaviour of existing structures, the capabilities of different methods to determine the actual residual stresses in the laminates have been explored.

Several methods based on instrumented indentation have been developed for local evaluation of residual stresses in metals and glasses on the basis of their influence on yield stress and/or on the size of the cracks produced by sharp indenters. Variations in these parameters originate changes in P-h curves revealing modifications in the contact areas and in the elastic penetration. However, it has been demonstrated that the residual stresses did not produce any appreciable change in the P-h curves in a series of alumina-zirconia laminates, making it impossible to use such methods<sup>51</sup> and, thus, evaluation of the residual stresses in ceramic laminates from indentation experiments requires the direct observation of the cracks<sup>18, 51, 52</sup>. Determinations of the variation of the indentation crack lengths as a function of the position of the indentations in the layers in alumina/zirconia laminates allowed the determination of the residual stress profile across the layers, which was in agreement with that calculated by the FEM for the surface of the materials<sup>18, 52</sup>. This method is limited to the characterisation of the surface of the material and the layers have to have sufficient width as to admit a series of non interacting indentations.

X-ray and neutron diffractions and spectroscopic analyses of photo-stimulated fluorescence or Raman spectra are being employed to determine residual stresses in monolithic materials and coatings. The X-ray diffraction gives clear information about the residual stresses at few microns from the surface of the pieces<sup>53</sup> while the neutron diffraction technique is suitable for characterising the bulk. Nevertheless, in general both kinds of emissions have not been used for the characterisation of laminates due to the difficulty of focussing the beams in the relatively thin layers. Moreover, neutron sources are not easy to reach neither to handle. Some preliminary studies are being performed in model alumina/zirconia laminates to establish the adequate methodology to study ceramic laminates using neutrons<sup>54</sup>.

The technique of piezo-spectroscopy using the chromophoric fluorescence of  $\text{Al}_2\text{O}_3$  was first applied by Grabner<sup>55</sup> to measure the residual stresses in monophase materials. This technique is also valid for Raman assessment and it has been applied to certain Raman bands of  $\text{ZrO}_2$ . A combination of both has allowed the complete characterisation of residual stresses in the fracture surfaces of indentation-strength  $\text{Al}_2\text{O}_3$ - $\text{ZrO}_2$  composites<sup>56</sup>.

After the first experiments performed by de Portu et al<sup>57</sup>, piezo-spectroscopy has been successfully applied to determine the residual stress distribution in alumina-based laminates and compared to those calculated analytically and by FEM<sup>47, 48, 50-52</sup>. Good agreements have been found using for calculations the Young modulus and the actual strains during cooling from the sintering temperature, determined by dilatometry, of monoliths with the composition of the layers and processed in the same way. For  $\text{Al}_2\text{O}_3/\text{Al}_2\text{TiO}_5$  specimens designed on the basis of crack-deflecting interfaces<sup>47</sup>, extremely low levels of stresses that agreed with the analytically calculated ones

were detected. Compressive residual stresses ( $\approx 20\text{MPa}$ ) were practically constant in the thick external and central load bearing  $\text{Al}_2\text{O}_3$  layers while tensile stresses changed sharply through the crack deflecting  $\text{Al}_2\text{O}_3/\text{Al}_2\text{TiO}_5$  internal layers from the maximum values ( $\approx 20\text{MPa}$ ) at the layers interfaces to minimum values ( $\approx 5\text{MPa}$ ) at their centres. For  $\text{Al}_2\text{O}_3/\text{ZrO}_2$  specimens designed for strengthening with external layers in compression<sup>47, 50</sup> the experimental distribution of residual stresses was similar to that calculated by FEM for the surface of the specimens. For symmetric specimens the residual stresses varied within each internal layer with a parabolic trend, from minimum absolute values at their centres to maximum absolute values at the interfaces; compressive residual stresses decreased towards the surface of the specimens. Maximum absolute values were coincident with those analytically calculated. Asymmetries in the width of the external layers originated changes in the stress distribution, especially in the external layers.

### 3. EFFECT OF THE RESIDUAL STRESSES IN THE MECHANICAL BEHAVIOUR OF CERAMIC LAMINATES

As schematized in figure 4, once cooled from the sintering temperature, the different layers of a laminate will remain in compression or tension depending on their relative thermal strains. The laminates are extremely anisotropic structures which mechanical behaviour is usually optimized under flexure with the load perpendicular to the planes of the layers (Fig. 5 a) even though some studies have also been performed for loads parallel to the layers and defects contained in the internal layers (Fig. 5 b).

Moreover, components usually fail from defects present at the surfaces because of their higher severity for similar sizes and shapes. Therefore, cracks contained in the outer layers of laminates under loads perpendicular to the layers will be mostly considered in the following discussion. The case of load parallel to the layers will also be discussed for the studied cases.

#### 3.1 Laminates with outer layers in compression

When the outer layers of laminate present lower thermal strains than the internal ones, compressive stresses are developed within the outer layers when the structure is cooled from the sintering temperature (Fig. 4 a and c). This laminate design approach is the so called strengthening approach because the laminates present increased strength, as compared to that of monoliths with the same microstructure as that of the external layers. Examples of this kind of laminates are shown in figure 2. For the loading configuration in figure 5 a, a crack present in the outer layers will propagate when the stress intensity factor at the tip of the crack overcomes the critical stress intensity factor of the outer layer. For a crack of depth "c" that grows under an externally applied stress and in a residual stress field, the apparent critical stress intensity factor of the external layer,  $\overline{K}_{\text{appt}}$ , is given by:

$$\overline{K}_{\text{appt}} = K_c - K_r \quad (5)$$

being  $K_c$  the critical stress intensity factor of the residual stress free material and  $K_r$  the stress intensity factor due to

the residual stress field. In the case of compressive stresses in the external layer,  $K_1$  is negative and an apparent increment in the toughness of the material together with an increase of fracture strength<sup>15, 25, 51, 58</sup> and associated properties<sup>59-61</sup> are observed. For the laminate to be in equilibrium, a certain level of compressive stresses in the external layers is tied to the presence of tensile stresses which level depend on their thickness in the internal layers. Thus, this latter has to be tailored in order to impede the generation of the so called tunnelling cracks that traverse the internal layers and can lead to the failure of the structure<sup>62, 63</sup>.

Figure 2 shows two laminates designed on the basis of results plotted in figure 3 b to reach two different distributions of residual stresses according to eqs. (2) and (3). Both laminates alternated layers of the same thickness of alumina with 5vol.% of YTZP (A5Z, dark), under compression, with layers of alumina with 40vol.% of YTZP (A40Z, bright), in tension. The laminates were fabricated by alternate stacking of green tapes of the two compositions and cold pressing and the sintering schedule was selected on the basis of the sintering behaviour of the two compositions<sup>15, 26</sup>. According to eqs. (2) and (3), upper limits for the residual stresses within the laminate with similar layer thicknesses (figure 2 a) would be -268 MPa and 241 MPa whereas for the laminate with the thinnest tensile layers (Fig. 2 b) these values would be -187 MPa and 213 MPa for A5Z and A40Z layers, respectively<sup>15</sup>. Experimental determinations by piezospectroscopy of the stress distribution through cross sections of bars ( $3 \times 4 \times 27 \text{ mm}^3$ ) of laminate in figure 2 b showed that the stress varied across the layers from the highest values measured at the interfaces between the layers towards their centres. This stress distribution was similar to that calculated for the surface of the specimen by the Finite Element Method (FEM)<sup>50</sup> and the maximum values experimentally measured ( $\sim -140$  and  $220 \text{ MPa}$ ) were in the range of those calculated ( $-120$  and  $240 \text{ MPa}$  for A and A40Z, respectively).

The fracture strength data recorded for bars of laminates shown in figure 2, loaded in four points bending with the

load parallel to the planes of the layers and with indentations in the external layer under tension, are plotted in figure 5. For comparative purposes the same plot for a monolithic material with the same composition as the external layers, A5Z, is presented. Two points have to be highlighted. First one is the clear difference that exists between the slopes corresponding to the monolithic and the laminate specimens. The lower values for the laminates reveal their R-curve behaviour during fracture and, consequently, a lower dependence of the strength on the size of the critical defects. This R-curve behaviour has also been proved for similar alumina-zirconia materials<sup>37</sup> and its influence in the strength distribution has been analyzed<sup>38</sup>. The second aspect is that values obtained for laminate in figure 2 b are about 20% higher than those corresponding to laminate in figure 2 a, being this value similar to the relative difference in the level of compressive stresses predicted from eqs. (2) and (3) for the laminates ( $\approx 30\%$ ). It is necessary to remark that, for the strengthening mechanism to be efficient certain conditions for the size and location of the defects with respect to the residual stress distribution exist. In fact, it has been observed in glasses and ceramics that reinforcement can be optimised by moving the maxima of the compressing stress distribution to a point located at a specific distance beneath the surface of the laminate subjected to tensile stresses during flexure<sup>64, 65</sup>.

### 3.2 Laminates with the internal layers in compression

As it has been discussed previously the design of laminates can also be done to develop the compressive residual stresses in the layers located inside the structure (Fig. 4 b). In general, such layers are designed relatively thin in order to diminish the associated level of tensile stresses in the outer layers. Depending on the relative orientation of the applied load and of the planes of the layers (Fig. 5) the main phenomena acting during fracture of laminates with internal compressive layers are crack bifurcation and crack arrest at the compressive

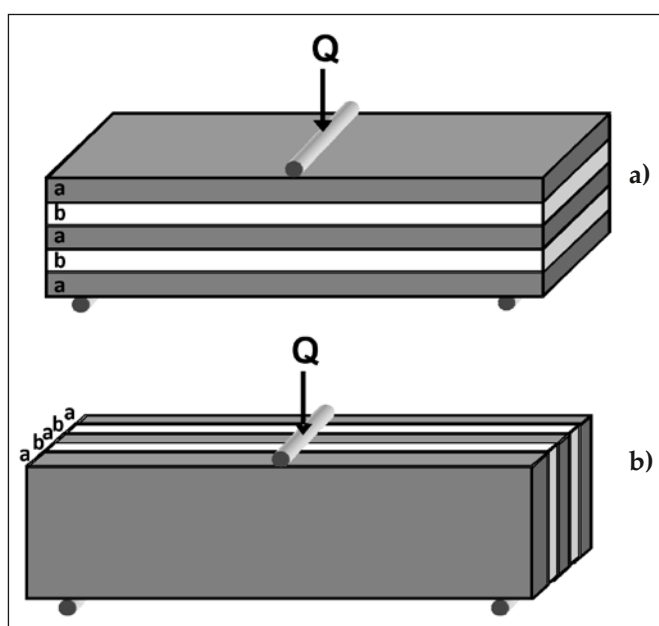


Figure 5. Flexure loading configurations for laminates. a) Load direction perpendicular to the planes of the layers. b) Load direction parallel to the planes of the layers.

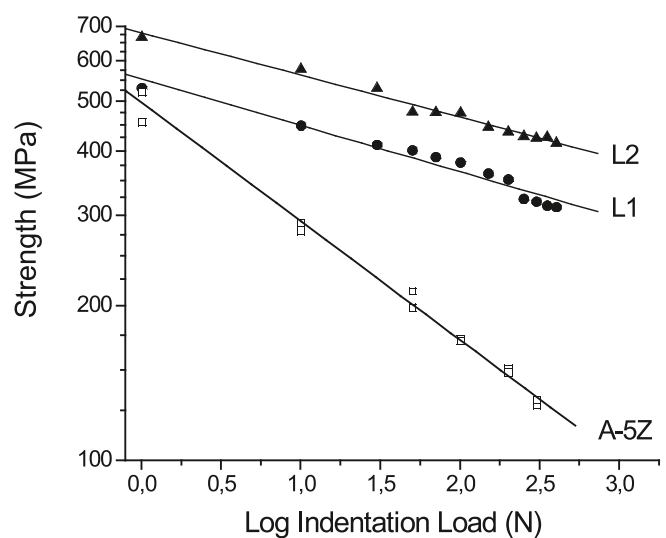


Figure 6 fracture strength of indented specimens as a function of the indentation load. The laminated structures L1 and L2 are shown in figures 2 a and 2 b, respectively. Data for monolithic specimens of the same composition as that of the external layers, A5Z, are also shown for comparison. The influence of the residual stresses in the values of the slope and the absolute strength values for L1 and L2 is apparent<sup>15</sup>.

layers. In this kind of laminates the existence of threshold strength values have been reported<sup>18, 41</sup>.

The phenomenon of crack bifurcation was first demonstrated for a laminate made of three thin layers of Al<sub>2</sub>O<sub>3</sub> sandwiched between four much thicker ZrO<sub>2</sub> (12mol% CeO<sub>2</sub>) layers<sup>16</sup>. Such structure presented high compressive stresses (≈2 GPa) within the Al<sub>2</sub>O<sub>3</sub> layers due to the differences in the thermal expansion coefficients of the layers. In addition, the corresponding tensile stresses in the thick external ZrO<sub>2</sub> (12mol% CeO<sub>2</sub>) were negligible.

The stress state schematized in figure 4 b, derived from the simple model of a plate in which the different layers are subjected to biaxial stress states, occurs only in the bulk of the laminate. To explain the bifurcation phenomena it is necessary to take into account the tri-axial stress state at and near the free surface. It has been shown that an out of plane tensile component that rapidly decreases with depth into the bulk appears in this region (Fig. 7 a). For thicknesses of the compressed layer higher than a critical one, (*t<sub>c</sub>*), a crack running along the middle plane of the compressed layer at its surface which is called edge crack is formed due this tensile stress component. The critical thickness is given by<sup>16</sup>:

$$t_c = \frac{G_c \cdot E}{0.34 \cdot (1 - \nu^2) \sigma_r^2} \quad (6)$$

where *G<sub>c</sub>* and *ν* are the critical strain energy release rate and the Poisson's coefficient of the material constituent of the layer and *σ<sub>r</sub>* is the level of compressive residual stresses at the centre of the layer.

When a crack propagates through the laminate two new free surfaces are created and when these surfaces reach the layer under compression (Fig 7.b) the stresses state changes due to the tensile stress created at the free surfaces. This new stress state originates the bifurcation of the crack into two new cracks that run parallel to the layer (Figure 7.c) until new cracks perpendicular to the layer are created by the combined action of the external load and the defects present in the material. This fracture mode proceeds until the complete failure of the laminate which macroscopically presents non-catastrophic failure<sup>16, 30, 42</sup>. The phenomenon of crack bifurcation is still an open subject; as analysis posterior to this first one proposed reveal certain discrepancies for this explanation<sup>66, 67</sup>.

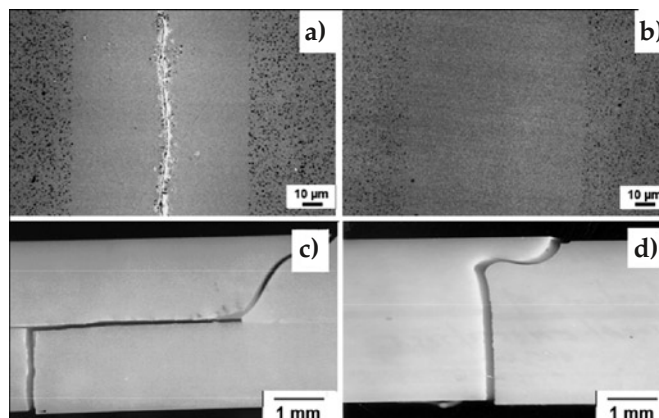


Figure 8. ZrO<sub>2</sub>-ZrO<sub>2</sub> sandwich laminates designed with compressive stresses in the thin internal layers<sup>30</sup>.

- a) Cross section of a laminate with high compressive stresses. The edge crack is observed. SEM.
  - b) Cross section of a laminate with high compressive stresses. No edge crack is observed. SEM.
  - c) Fracture behaviour of laminate (a). Crack bifurcation is observed. Optical microscopy.
  - d) Fracture behaviour of laminate (b). No crack bifurcation is observed. Optical microscopy.
- The tensile surfaces in figures c and d are located at the lower part of the micrographs.

The influence of the design variables on the phenomena of crack bifurcation and edge cracking has been systematically studied for different laminates designed on the basis of zirconia transformation<sup>30, 41, 42</sup>. Different magnitudes of residual stresses have been obtained by tailoring the levels of thermal expansion mismatch and the layer thicknesses to reach the corresponding strains. Sequential slip casting has been used as green processing method to control the compositional homogeneity and the thickness of the different layers.

A series of laminates were fabricated from green bodies that contained thin layers (5 to 200 μm thick) of a mixture of pure monoclinic ZrO<sub>2</sub> powder (MZ) with a tetragonal ZrO<sub>2</sub> powder stabilised with 3 mol% Y<sub>2</sub>O<sub>3</sub> (YTZP), sandwiched between two thick layers (1-2 mm thick) of YTZ powder containing 5 vol.% of Al<sub>2</sub>O<sub>3</sub>. Figure 8 a-b shows the cross section of two of those materials<sup>30</sup>. Both of them are constituted by two outer thick (1500μm) layers of YTZP with 5vol.% of Al<sub>2</sub>O<sub>3</sub>.

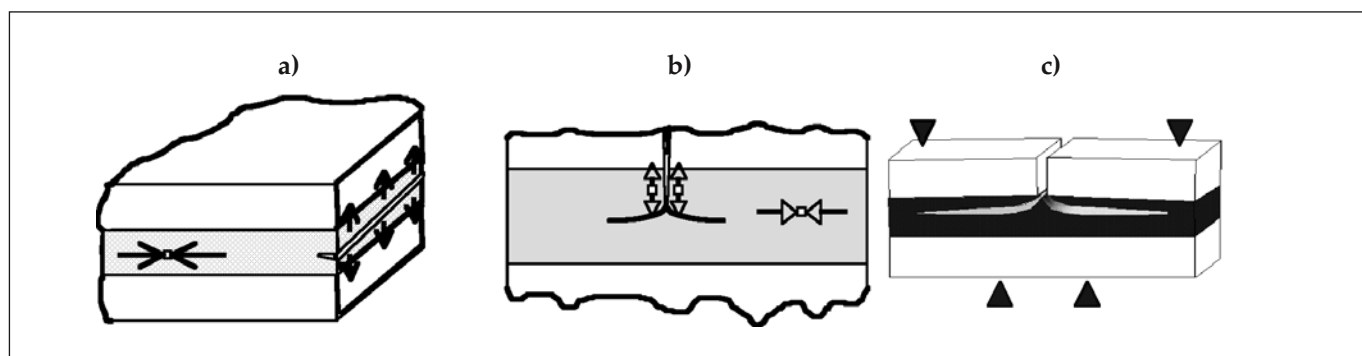


Figure 7. Schematic representation of the crack bifurcation process in laminates. a) Stress state at the centre of for an internal layer under compression and tensile stresses at the edge of a free surface in an internal layer under compression. b) When a crack reaches the internal layer under compression it generates a new surface in tension. c) Bifurcation of the crack.

and one inner thin (100 $\mu\text{m}$ ) layer. They presented different levels of compressive residual stresses due to differences in the composition of the thin layers. The total amount of  $\text{Y}_2\text{O}_3$  resulting from different mixtures of pure monoclinic  $\text{ZrO}_2$  and YTZP determined the transformability of  $\text{ZrO}_2$  in the thin layers. The thin layer containing the lowest amount of  $\text{Y}_2\text{O}_3$  (1.2 mol%) would tend to expand more on cooling due to the tetragonal-monoclinic transformation of zirconia than the one with the highest amount of stabilizer (2 mol%). Then, residual stresses were higher in the laminate in which the thin layer contained the lowest amount of  $\text{Y}_2\text{O}_3$  (1.2 mol%, fig. 8 a, c). The laminate with the highest residual stresses showed edge crack in the middle of the thin compressed layer (figure 8 a) while no edge crack was observed in the laminate with lower residual stresses (figure 8 b). Moreover, crack bifurcation during four point bending tests was observed in the specimens containing edge cracks (Figs. 8 c) while bifurcation did not occur in the specimens without edge crack (8 d).

This association of edge crack at the free surfaces and bifurcation has been also reported for alumina-zirconia laminates designed on the basis of thermal expansion mismatch

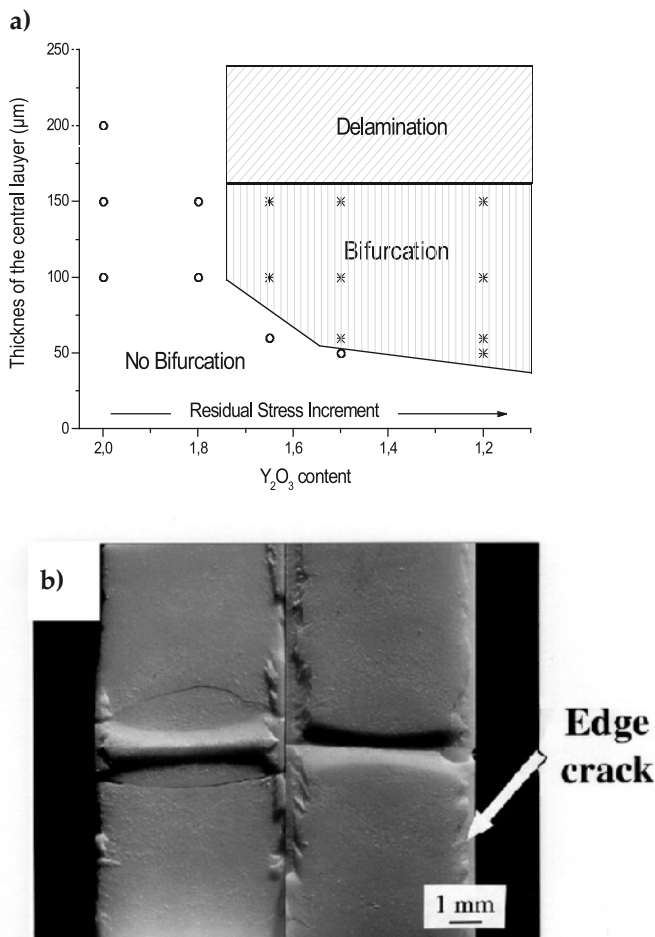


Figure 9.  $\text{ZrO}_2$ -  $\text{ZrO}_2$  sandwich laminates designed with compressive stresses in the thin internal layers. The thick layers were composed of YTZP and the thin ones had different amounts of monoclinic zirconia<sup>30</sup>.

a)  $\text{Y}_2\text{O}_3$  content vs thickness of the central layer. The regions for which bifurcation and no bifurcation have been observed in laminates are shown.

b) Fracture surface of a laminate showing the elevation associated to bifurcation and the edge cracks at both sides. SEM micrograph.

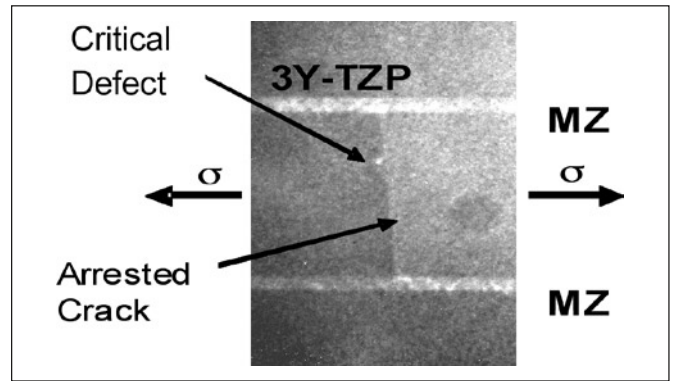


Figure 10. Surface in tension of a laminar ceramic composed of thick YTZP (1 mm) layers and thin (100  $\mu\text{m}$ ) monoclinic zirconia, MZ, layers. The arrest by the compressive layers of the natural flaw that acted as critical defect is observed.

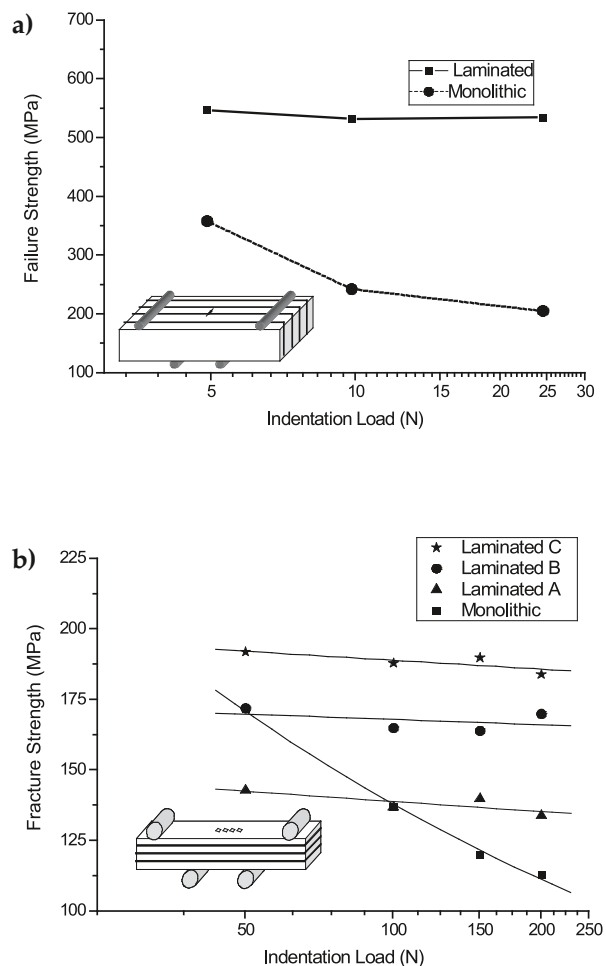


Figure 11.- Fracture strength of indented laminates with internal compressive layers and of indented monoliths with the same composition as that of the external layers. The occurrence of the threshold stress and the R curve behaviour is observed.

a) Laminated specimens with thick ( $\approx 315\mu\text{m}$ , white) layers of alumina+5vol.% YTZP, A5Z, and thin ( $\approx 29\mu\text{m}$ , black) layers of monoclinic zirconia, MZ, + 5 vol.% alumina, tested with the load direction parallel to the planes of the layers<sup>41</sup>.

b) Laminated specimens with thick ( $\approx 315\mu\text{m}$ , white) layers of alumina+5vol.% YTZP, A5Z, and thin (150, 90, and  $60\mu\text{m}$  for A, B and C, respectively) layers of alumina + 30vol.% of MZ tested with the load direction perpendicular to the planes of the layers<sup>18</sup>.

due to zirconia transformation<sup>18, 24, 41, 42</sup>. As it is shown in figure 9 a as the thickness of the central layer or the residual stress (in terms of the  $Y_2O_3$  content) decreases, the fracture mode changes from delamination to bifurcation and to no special fracture features. The fracture surface of a laminate with internal compressive stresses showing the elevation associated to bifurcation and the edge cracks at both sides is shown in figure 9 b.

The occurrence of bifurcation strongly changes the crack direction and running distance, avoiding the catastrophic fracture of the piece. However, the most important characteristic of laminates with internal layers subjected to highly compressive stresses is that the crack arrest by the compressive layers leads to a threshold strength for the failure of the structure. Figure 10 shows the crack arrest phenomena observed in a laminate that alternates thin layers (100 $\mu$ m) of unstabilised zirconia (MZ) with thick layers (1 mm) of YTZP. During cooling from the sintering temperature the tetragonal-monoclinic transformation of the unstabilised zirconia constituent of the thin layers would lead to a volume expansion of the layers of about 3%. This expansion is impeded by the thick stabilised layers which exert compression on the thin layers. A natural flaw that acts as critical defect propagated through the YTZP layer due to the external tensile stress applied to the sample during bending test and was arrested between the two compressive layers. A flaw of such size ( $\approx$ 1mm) will be responsible of a significant fracture strength decrease (higher than 50%). But in this case insensitiveness to the flaw size was observed, and after crack arrest increasing load had to be applied to continue the fracture process, indicating that residual stresses developed threshold strength in the material.

The above described reinforcement mechanisms in the  $ZrO_2$ - $ZrO_2$  laminate have been confirmed to be effective other systems such as alumina-mullite<sup>17</sup> and alumina-zirconia<sup>18, 41</sup>.

Figure 11 shows the results of indentation-strength tests for laminates with thin compressive internal layers. Tests were performed with the plane of the layers oriented both parallel and perpendicular to that of the applied load and both configurations showed independence of the strength with the initial flaw size, determined by the indentation load.

In figure 11 a, results for specimens constituted by thick A5Z layers and monoclinic zirconia thin layers<sup>41</sup> together with those for a monolithic material of the same composition as the external layers, plotted for comparison, are shown.

Figure 11 b shows a similar plot for laminates with different thicknesses (150, 90 and 60 $\mu$ m) of the compressive layers. The dependence of the threshold strength with the thickness of the compressive layers is apparent. The fracture mechanics analysis<sup>17</sup> allows the determination of the stress intensity function by superimposing the two stress fields (external stress of bending and residual stress) and defined the threshold stress below which the laminate will not fail by:

$$\sigma_{thr} = \frac{K_c}{\sqrt{\pi \frac{t_2}{2} \left(1 + \frac{2t_1}{t_2}\right)}} + \sigma_c \left(1 - \left(1 + \frac{t_1}{t_2}\right) \frac{2}{\pi} \sin^{-1} \left( \frac{1}{1 + \frac{2t_1}{t_2}} \right)\right) \quad (7)$$

where  $K_c$  is the fracture toughness of the thin layer,  $t_1$  and  $t_2$  are the thicknesses of the thin and thick layers respectively, and  $\sigma_c$  is the residual compressive stress. Equation 7 shows that  $\sigma_{thr}$  increases with the toughness, the compressive stresses and the thickness of the thin layers. In fact it has been observed that crack interacting very thin layers (1  $\mu$ m) under compression, do not change the crack path or the crack length<sup>23</sup>. It should be noted that equation 7 is only derived for the case of loads applied parallel to the layer plane (Fig. 5 b). For the other case, the weight function method can be used to estimate a threshold strength<sup>49, 67, 68</sup>.

#### 4. CONCLUDING REMARKS

The works presented here prove that fracture behaviour of ceramic materials can be significantly improved by the layered structure design. In particular, the tailoring of the thickness and location of layers in compression can lead to extremely performing structures in terms of strength values and reliability. External layers in compression increase the apparent fracture toughness and, consequently, strengthening of the structure takes place. When relatively thin and highly compressed layers are located inside the material, crack bifurcation, crack arrest and threshold strength during fracture occur.

#### ACKNOWLEDGEMENTS

This work has been supported by the Spanish Government under contracts MEC MAT2006-01038 and MAT2006-13480.

#### REFERENCES

- [1] K. E. Gunnison, M. Sarikaya, J. Liu and I. A. Aksay, "Structure-mechanical property relationships in a biological ceramic-polymer composite: nacre." Proceedings of *Hierarchically structured materials*, Pittsburgh, Penn. USA, I. A. Aksay, E. Baer, M. Sarikaya and D. Tirrel. Eds., Materials Research Society, 1992, p. 171-183.
- [2] I. A. Aksay and M. Sarikaya, "Bioinspired processing of composite materials" Proceedings of *Ceramics toward the 21st century*. Tokyo, N. Soga and A. Kato, Eds., The Ceramic Society of Japan, 1991, p. 136-149.
- [3] W. J. Clegg, K. Kendall, N. M. Alford, T. W. Button and J. D. Birchall. "A Simple Way to Make Tough Ceramics", *Nature*, 347 (6292) 455-457 (1990).
- [4] H. M. Chan. "Layered ceramics: Processing and mechanical behavior". *Annu. Rev. Mater. Sci.*, 27 (1) 249-282 (1997).
- [5] M. Y. He and J. W. Hutchinson. "Crack Deflection at an Interface between Dissimilar Elastic-Materials". *Int. J. Solids. Struct.*, 25 (9) 1053-1067 (1989).
- [6] A. J. Phillippis, W. J. Clegg and T. W. Clyne. "Fracture-Behavior of Ceramic Laminates in Bending .1. Modeling of Crack-Propagation". *Acta Metall. Mater.*, 41 (3) 805-817 (1993).
- [7] S. Bueno and C. Baudin. "Flaw tolerant ceramic laminates with negligible residual stresses between layers". *Key Eng. Mater.*, 333 17-26 (2007).
- [8] J. Ma, H. Z. Wang, L. Q. Weng and G. E. B. Tan. "Effect of porous interlayers on crack deflection in ceramic laminates". *J. Eur. Ceram. Soc.*, 24 (5) 825-831 (2004).
- [9] N. Claussen and J. Steeb. "Toughening of Ceramic Composites by Oriented Nucleation of Microcracks". *J. Am. Ceram. Soc.*, 59 (9-10) 457-458 (1976).
- [10] S. Bueno and C. Baudin. "Design and processing of a ceramic laminate with high toughness and strong interfaces". *Compos. Pt. A-Appl. Sci. Manuf.*, 40 (2) 137-143 (2009).
- [11] B. Ferrari, A. Bartret and C. Baudin. "Sandwich materials formed by thick alumina tapes and thin-layered alumina-aluminium titanate structures shaped by EPD". *J. Eur. Ceram. Soc.*, 29 (6) 1083-1092 (2009).
- [12] B. Ferrari, S. Bueno and C. Baudin. "Consolidation of flaw-tolerant layered structures by the insertion of reactive layers". *Bol. Soc. Esp. Ceram. V.*, 48 (5) 261-266 (2009).
- [13] C. J. Russo, M. P. Harmer, H. M. Chan and G. A. Miller. "Design of a Laminated Ceramic Composite for Improved Strength and Toughness". *J. Am. Ceram. Soc.*, 75 (12) 3396-3400 (1992).

- [14] S. Bueno, R. Moreno and C. Baudin. "Design and processing of  $\text{Al}_2\text{O}_3$ - $\text{Al}_2\text{TiO}_5$  layered structures". *J. Eur. Ceram. Soc.*, 25 (6) 847-856 (2005).
- [15] J. Gurauskis, A. J. Sanchez-Herencia and C. Baudin. "Alumina-zirconia layered ceramics fabricated by stacking water processed green ceramic tapes". *J. Eur. Ceram. Soc.*, 27 (2-3) 1389-1394 (2007).
- [16] M. Oechsner, C. Hillman and F. F. Lange. "Crack bifurcation in laminar ceramic composites". *J. Am. Ceram. Soc.*, 79 (7) 1834-1838 (1996).
- [17] M. P. Rao, A. J. Sanchez-Herencia, G. E. Beltz, R. M. McMeeking and F. F. Lange. "Laminar ceramics that exhibit a threshold strength". *Science*, 286 (5437) 102-105 (1999).
- [18] R. Bermejo, Y. Torres, A. J. Sanchez-Herencia, C. Baudin, M. Anglada and L. Llanes. "Residual stresses, strength and toughness of laminates with different layer thickness ratios". *Acta Mater.*, 54 (18) 4745-4757 (2006).
- [19] R. J. Moon, M. Hoffman, K. Bowman and K. Trumble. "Layer orientation effects on the R-curve behavior of multilayered alumina-zirconia composites". *Compos. Pt. B-Eng.*, 37 (6) 449-458 (2006).
- [20] R. Bermejo, Y. Torres and L. Llanes. "Loading configuration effects on the strength reliability of alumina-zirconia multilayered ceramics". *Comp. Sci. Tech.*, 68 (1) 244-250 (2008).
- [21] F. F. Lange. "Powder Processing Science and Technology for Increased Reliability". *J. Am. Ceram. Soc.*, 72 (1) 3-15 (1989).
- [22] A. J. Sanchez-Herencia. "Water based colloidal processing of ceramic laminates". *Key Eng. Mater.*, 333 39-48 (2007).
- [23] I. Nicolaidis, J. Gurauskis, C. Baudin, R. Moreno and A. J. Sanchez-Herencia. "Forming of ceramic laminates comprising thin layers of a few particles". *J. Am. Ceram. Soc.*, 91 (7) 2124-2129 (2008).
- [24] R. Bermejo, C. Baudin, R. Moreno, L. Llanes and A. J. Sanchez-Herencia. "Processing optimisation and fracture behaviour of layered ceramic composites with highly compressive layers". *Compos. Sci. Technol.*, 67 (9) 1930-1938 (2007).
- [25] V. M. Sglavo, M. Paternoster and M. Bertoldi. "Tailored residual stresses in high reliability alumina-mullite ceramic laminates". *J. Am. Ceram. Soc.*, 88 (10) 2826-2832 (2005).
- [26] A. J. Sanchez-Herencia, J. Gurauskis and C. Baudin. "Processing of  $\text{Al}_2\text{O}_3$ /Y-TZP laminates from water-based cast tapes". *Compos. Pt.B-Eng.*, 37 (6) 499-508 (2006).
- [27] J. B. Davis, A. Kristofferson, E. Carlstrom and W. J. Clegg. "Fabrication and crack deflection in ceramic laminates with porous interlayers". *J. Am. Ceram. Soc.*, 83 (10) 2369-2374 (2000).
- [28] M. Jiménez-Melendo, C. Clauss, A. Domínguez-Rodríguez, G. de Portu, E. Roncari and P. Pinasco. "High temperature plastic deformation of multilayered YTZP/ZTA composites obtained by tape casting". *Acta Mater.*, 46 (11) 3995-4004 (1998).
- [28] D. B. Marshall, J. J. Ratto and F. F. Lange. "Enhanced Fracture-Toughness in Layered Microcomposites of Ce-ZrO<sub>2</sub> and Al<sub>2</sub>O<sub>3</sub>". *J. Am. Ceram. Soc.*, 74 (12) 2979-2987 (1991).
- [30] A. J. Sanchez-Herencia, C. Pascual, J. He and F. F. Lange. " $\text{ZrO}_2/\text{ZrO}_2$  layered composites for crack bifurcation". *J. Am. Ceram. Soc.*, 82 (6) 1512-1518 (1999).
- [31] J. Requena, R. Moreno and J. S. Moya. "Alumina and Alumina Zirconia Multilayer Composites Obtained by Slip Casting". *J. Am. Ceram. Soc.*, 72 (8) 1511-1513 (1989).
- [32] P. S. Nicholson, P. Sarkar and X. Huang. "Electrophoretic Deposition and Its Use to Synthesize  $\text{ZrO}_2/\text{Al}_2\text{O}_3$  Micro-Laminate Ceramic-Ceramic Composites". *J. Mater. Sci.*, 28 (23) 6274-6278 (1993).
- [33] B. Ferrari, A. J. Sanchez-Herencia and R. Moreno. "Electrophoretic forming of  $\text{Al}_2\text{O}_3$ /Y-TZP layered ceramics from aqueous suspensions". *Mater. Res. Bull.*, 33 (3) 487-499 (1998).
- [34] B. Ferrari, S. Gonzalez, R. Moreno and C. Baudin. "Multilayer coatings with improved reliability produced by aqueous electrophoretic deposition". *J. Eur. Ceram. Soc.*, 26 (1-2) 27-36 (2006).
- [35] I. M. Low, R. D. Skala and D. S. Perera. "Fracture Properties of Layered Mullite Zirconia-Toughened Alumina Composites". *J. Mater. Sci. Lett.*, 13 (18) 1334-1336 (1994).
- [36] C. E. P. Willoughby and J. R. G. Evans. "The preparation of laminated ceramic composites using paint technology". *J. Mater. Sci.*, 31 (9) 2333-2337 (1996).
- [37] C. R. Chen, J. Pascual, F. D. Fischer, O. Kolednik and R. Danzer. "Prediction of the fracture toughness of a ceramic multilayer composite - Modeling and experiments". *Acta Mater.*, 55 (2) 409-421 (2007).
- [38] J. Pascual, T. Lube and R. Danzer. "Fracture statistics of ceramic laminates strengthened by compressive residual stresses". *J. Am. Ceram. Soc.*, 28 (8) 1551-1556 (2008).
- [39] D. J. Green, P. Z. Cai and G. L. Messing. "Residual stresses in alumina-zirconia laminates". *J. Eur. Ceram. Soc.*, 19 (13-14) 2511-2517 (1999).
- [40] P. Z. Cai, D. J. Green and G. L. Messing. "Mechanical characterization of  $\text{Al}_2\text{O}_3/\text{ZrO}_2$  hybrid laminates". *J. Eur. Ceram. Soc.*, 18 (14) 2025-2034 (1998).
- [41] M. G. Pontin, M. P. Rao, A. J. Sanchez-Herencia and F. F. Lange. "Laminar ceramics utilizing the zirconia tetragonal-to-monoclinic phase transformation to obtain a threshold strength". *J. Am. Ceram. Soc.*, 85 (12) 3041-3048 (2002).
- [42] A. J. Sanchez-Herencia, L. James and F. F. Lange. "Bifurcation in alumina plates produced by a phase transformation in central, alumina/zirconia thin layers". *J. Eur. Ceram. Soc.*, 20 (9) 1297-1300 (2000).
- [43] R. A. Cutler, J. D. Bright, A. V. Virkar and D. K. Shetty. "Strength Improvement in Transformation-toughened Alumina by Selective Phase Transformation". *J. Am. Ceram. Soc.*, 70 (10) 714-718 (1987).
- [44] R. Krishnamurthy and B. W. Sheldon. "Stresses due to oxygen potential gradients in non-stoichiometric oxides". *Acta Mater.*, 52 (7) 1807-1822 (2004).
- [45] O. Sbaizero and E. Lucchini. "Influence of residual stresses on the mechanical properties of a layered ceramic composite". *J. Eur. Ceram. Soc.*, 16 (8) 813-818 (1996).
- [46] T. Chartier, D. Merle and J. L. Besson. "Laminar Ceramic Composites". *J. Eur. Ceram. Soc.*, 15 (2) 101-107 (1995).
- [47] G. de Portu, J. Gurauskis, L. Micele, A. J. Sanchez-Herencia, C. Baudin and G. Pezzotti. "Piezo-spectroscopic characterization of alumina-zirconia layered composites". *J. Mater. Sci.*, 41 (12) 3781-3785 (2006).
- [48] G. de Portu, S. Bueno, L. Micele, C. Baudin and G. Pezzotti. "Piezo-spectroscopic characterization of alumina-aluminium titanate laminates". *J. Eur. Ceram. Soc.*, 26 (13) 2699-2705 (2006).
- [49] R. Bermejo, J. Pascual, T. Lube and R. Danzer. "Optimal strength and toughness of  $\text{Al}_2\text{O}_3$ -ZrO<sub>2</sub> laminates designed with external or internal compressive layers". *J. Eur. Ceram. Soc.*, 28 (8) 1575-1583 (2008).
- [50] J. Gurauskis. "Desarrollo de materiales laminados de alumina-circona reforzados por tensiones residuales" Ph.D. memory. Universidad Autónoma de Madrid, Madrid, 2006.
- [51] E. Jimenez-Pique, L. Ceseracciu, Y. Gaillard, M. Barch, G. De Portu and M. Anglada. "Instrumented indentation on alumina-alumina/zirconia multilayered composites with residual stresses". *Philos. Mag.*, 86 (33-35) 5371-5382 (2006).
- [52] H. Moon, J. H. Bahk and F. F. Lange. "Threshold strength and residual stress analysis of zirconia-alumina laminates". *Int. J. Mater. Res.*, 98 674-682 (2007).
- [53] O. Kesler, J. Matejicek, S. Sampath, S. Suresh, T. Gnaeupel-Herold, P. C. Brand and H. J. Prask. "Measurement of residual stress in plasma-sprayed metallic, ceramic and composite coatings". *Mater. Sci. Eng.-A; Struct. Mater. Prop.*, 257 (2) 215-224 (1998).
- [54] J. Ruiz-Hervias, G. Bruno, J. Gurauskis, A. J. Sanchez-Herencia and C. Baudin. "Residual stresses in  $\text{Al}_2\text{O}_3/\text{Y-TZP}$  ceramic laminates fabricated by tape and slip casting". *Proceedings of Materials Science Forum, Volume: 571-572*, 2008, p. 327-332.
- [55] L. Grabner. "Spectroscopic Technique for Measurement of Residual-Stress in Sintered  $\text{Al}_2\text{O}_3$ ". *J. Appl. Phys.*, 49 (2) 580-583 (1978).
- [56] C. Baudin, J. Gurauskis, A. J. Sanchez-Herencia and V. M. Orea. "Indentation Damage and Residual Stress Field in Alumina-Y<sub>2</sub>O<sub>3</sub>-Stabilized Zirconia Composites". *J. Am. Ceram. Soc.*, 92 (1) 152-160 (2009).
- [57] G. de Portu, L. Micele, Y. Sekiguchi and G. Pezzotti. "Measurement of residual stress distributions in  $\text{Al}_2\text{O}_3/\text{3Y-TZP}$  multilayered composites by fluorescence and Raman microprobe piezo-spectroscopy". *Acta Mater.*, 53 (5) 1511-1520 (2005).
- [58] A. V. Virkar, J. L. Huang and R. A. Cutler. "Strengthening of Oxide Ceramics by Transformation-Induced Stresses". *J. Am. Ceram. Soc.*, 70 (3) 164-170 (1987).
- [59] G. de Portu, L. Micele, D. Prandstraller, G. Palombarini and G. Pezzotti. "Abrasive wear in ceramic laminated composites". *Wear*, 260 (9-10) 1104-1111 (2006).
- [60] E. Jimenez-Pique, L. Ceseracciu, M. Anglada, F. Chalvet and G. de Portu. «Hertzian fatigue in alumina/zirconia laminated composites». *Bol. Soc. Esp. Ceram. V.*, 44 (5) 307-312 (2005).
- [61] F. Toschi, C. Melandri, P. Pinasco, E. Roncari, S. Guicciardi and G. de Portu. «Influence of residual stresses on the wear behavior of alumina/alumina-zirconia laminated composites». *J. Am. Ceram. Soc.*, 86 (9) 1547-1553 (2003).
- [62] S. Ho and Z. Suo. "Tunneling Cracks in Constrained Layers". *J. Appl. Mech.-T. Asme*, 60 (4) 890-894 (1993).
- [63] R. Bermejo, A. J. Sanchez-Herencia, C. Baudin and L. Llanes. "Residual stresses in  $\text{Al}_2\text{O}_3$ -ZrO<sub>2</sub> multilayered ceramics: nature, evaluation and influence on the structural integrity". *Bol. Soc. Esp. Ceram. V.*, 45 (5) 352-357 (2006).
- [64] D. J. Green, R. Tandon and V. M. Sglavo. "Crack arrest and multiple cracking in class through the use of designed residual stress profiles". *Science*, 283 (5406) 1295-1297 (1999).
- [65] V. M. Sglavo and M. Bertoldi. "Design and production of ceramic laminates with high mechanical reliability". *Compos. Pt. B-Eng.*, 37 (6) 481-489 (2006).
- [66] K. Hbaieb, R. M. McMeeking and F. F. Lange. "Crack bifurcation in laminar ceramics having large compressive stress". *Int. J. Solids Struct.*, 44 (10) 3328-3343 (2007).
- [67] M. Lugovy, V. Slyunyayev, N. Orlovskaya, G. Blugan, J. Kuebler and M. Lewis. "Apparent fracture toughness of  $\text{Si}_3\text{N}_4$ -based laminates with residual compressive or tensile stresses in surface layers". *Acta Mater.*, 53 (2) 289-296 (2005).
- [68] R. Bermejo, Y. Torres, C. Baudin, A. J. Sanchez-Herencia, J. Pascual, M. Anglada and L. Llanes. "Threshold strength evaluation on an  $\text{Al}_2\text{O}_3$ -ZrO<sub>2</sub> multilayered system". *J. Eur. Ceram. Soc.*, 27 (2-3) 1443-1448 (2007).

Recibido: 15-11-2009  
 Aceptado: 20-12-2009